Palaeogeography, Palaeoclimatology, Palaeoecology 387 (2013) 153–164

Contents lists available at ScienceDirect

Palaeogeography, Palaeoclimatology, Palaeoecology

journal homepage: www.elsevier.com/locate/palaeo

# Mercury as a proxy for volcanic activity during extreme environmental turnover: The Cretaceous–Paleogene transition

A.N. Sial [a,*], L.D. Lacerda [b], V.P. Ferreira [a], R. Frei [c], R.A. Marquillas [d], J.A. Barbosa [e], C. Gaucher [f], C.C. Windmöller [g], N.S. Pereira [a]

[a] NEG-LABISE, Department of Geology, Federal University of Pernambuco, Recife, PE 50740-530, Brazil
[b] LABOMAR, Institute of Marine Sciences, Federal University of Ceará, Fortaleza 60165-081, Brazil
[c] Institute of Geography and Geology, University of Copenhagen, Oster Volgade 10, Copenhagen 1350, Denmark
[d] Universidad de Salta, CONICET, Buenos Aires 177, 4400 Salta, Argentina
[e] LAGESE, Department Geology, Federal University of Pernambuco, Recife 50740-530, Brazil
[f] Facultad de Ciencias, Universidad de La Republica, Montevideo, Uruguay
[g] Department of Chemistry, Federal University of Minas Gerais, Av. Antônio Carlos 6627, Belo Horizonte, Minas Gerais 31270-901, Brazil

ARTICLE INFO

*Article history:*
Received 8 February 2013
Received in revised form 12 July 2013
Accepted 18 July 2013
Available online 26 July 2013

*Keywords:*
Cretaceous–Paleogene transition
Volcanism
Mercury
Thermo-desorption
Carbon isotope stratigraphy

ABSTRACT

The usually low geological background concentrations of Hg makes this trace element suitable for identifying accumulation pulses in sediments that can be tentatively related to weathering processes and thus to climatic changes. Intense volcanism has witnessed the Cretaceous–Paleogene transition (KTB) and was, perhaps, responsible for dramatic climatic changes and decrease in biodiversity and mass extinction. We have used Hg concentrations as a proxy for volcanic activity and atmospheric Hg and $CO_2$ buildup across the KTB at three localities. In the Salta Basin, Argentina, Hg contents display several spikes across the KTB, with a maximum value of 250 $ng \cdot g^{-1}$. In three drill cores across the KTB in the Paraíba Basin, northeastern Brazil, Hg contents increase from the late Maastrichtian to early Danian and Hg spikes predate the KTB, perhaps, as a record of volcanic activity before (but very close to) this transition. At Stevns Klint, Denmark, Hg contents reached almost 250 $ng \cdot g^{-1}$ within a 5 cm thick-clay layer, the Fiskeler Member ('Fish Clay') that comprises the KTB. Some co-variation between Hg and $Al_2O_3$ contents has been observed in all of the studied sections across the KTB, suggesting that Hg is probably adsorbed onto clays. Thermo-desorption experiments in selected samples from the Yacoraite Formation showed $Hg^{+2}$ as the major species present, which is in agreement with a volcanic origin. Combined Hg and C-isotope chemostratigraphy may become a powerful tool for the eventual assessment of the role of volcanic activity during extreme climatic and biotic events, such as those during the KTB.



## 1. Introduction

Enrichment of mercury in the upper crust involves mobilization from mercury-bearing source rocks, transportation by hydrothermal fluids, deposition in chemical traps (ore deposits), and dispersal into adjacent and overlying lithosphere, hydrosphere and atmosphere (Barnes and Seward, 1997; Rytuba, 2005; Smith et al., 2008). The way Hg is delivered to the upper crust and ultimately to the surface environments includes a wide range of geochemical and environmental processes, including vaporization during its migration (Varekamp and Buseck, 1986; Varekamp and Waibel, 1987; Pyle and Mather, 2003; Smith et al., 2008). In sedimentary rocks, Hg can be present in sulfide minerals, adsorbed onto clays, incorporated into organic matter, and dissolved in hydrocarbons (Krupp, 1988).

The association of higher contents of Hg with modern carbonates finely inter-layered with terrigenous sediments may have ultimately resulted from increased atmospheric Hg deposition related to volcanism (Roos-Barraclough et al., 2002). The same association may have also occurred in the past (Nascimento-Silva et al., 2011). Leaching of this Hg from the land surface, and subsequent transport into the oceans, eventually could have led to the known accumulation of Hg in argillaceous carbonates. For example, higher Hg accumulation rates were found in sediments deposited after glacial maxima, when runoff is increased, than in sediment layers deposited before that, and it seems to represent a global phenomenon, as suggested by similar results obtained by the analysis of sediments in the Amazon region (Santos et al., 2001); Antarctica (Vandal et al., 1993) and Europe (Martínez-Cortizas et al., 1999).

Cataclysmic volcanoes have the potential of injecting enough Hg to the atmosphere to change global and regional Hg cycles. For example, volcanic emissions of Hg to the Earth's atmosphere between 1980 and 2000 have totaled about 90 $tons \cdot yr^{-1}$ (Nriagu and Becker, 2003).

* Corresponding author. Tel.: +55 81 2126 8243; fax: +55 81 2126 8242.
*E-mail address:* sial@ufpe.br (A.N. Sial).

0031-0182/$ – see front matter © 2013 Elsevier B.V. All rights reserved.
http://dx.doi.org/10.1016/j.palaeo.2013.07.019

Roos-Barraclough et al. (2002) found evidence of increasing Hg deposition in cores of lake sediments of the Swiss Jura Mountains, associated to known volcanic eruptions.

Sanei et al. (2012) associated increasing atmospheric Hg deposition with catastrophic Siberian Traps volcanic eruptions, followed by the disruption of the organic fixation of Hg and consequently increasing dissolved mercury fluxes. Nascimento-Silva et al. (2011) reported Hg chemostratigraphy from a drill hole in the Paraíba Basin, northeastern Brazil, with a positive Hg excursion in the Cretaceous–Paleogene transition (KTB) and suggested that this excursion was related to volcanism.

Besides a direct volcanic origin of Hg, higher Hg concentrations in the atmosphere could result from widespread reduction of biological activity that decreases or even shuts the scavenging and biological fixation of Hg from the atmosphere, increasing the dissolved Hg fluxes. Before a reduced bioproductivity, Hg would be less likely captured by organic matter, one of the major Hg sinks (Sanei et al., 2012).

It has been claimed that single/multiple meteorite impact(s) during the KTB contributed to greenhouse effect and global warming, which acted on an already damaged ecosystem. An alternative cause for dramatic environmental changes during the KTB is the intense volcanism related to the Deccan Traps (e.g. Hoffman et al., 2000). Correlation between large volcanic events and sudden environmental crises becomes evident from well-constrained age data for large igneous provinces (LIP) according to Kelley (2007). The effect of volcanism could be more globally widespread and its duration more timely representative than a meteorite hypervelocity impact.

Our study aims at contributing to this discussion by proposing that Hg, as a volcanogenic trace element, could potentially help in identifying whether or not volcanism was significantly responsible for a climatic reorganization during the KTB. We focus on Hg concentration fluctuations in the following carbonate formations bracketing the KTB: (a) Salta Basin (Yacoraite and Olmedo formations), northwestern Argentina, (b) Paraíba Basin (Gramame and Maria Farinha formations), northeastern Brazil, and (c) Danish Basin at Stevns Klint, Denmark (Højerup and Fiskeler members).

## 2. The Cretaceous–Paleogene transition

The mass extinction recorded in the KTB is generally regarded as a consequence of single (e.g. Alvarez et al., 1980; Claeys et al., 2002) or multiple meteorite impacts (e.g. Keller et al., 2003; Stüben et al., 2005) and/or of intense volcanic eruptions (e.g. Hoffman et al., 2000; Keller, 2005; Archibald et al., 2010). The hypothesis of Alvarez et al. (1980) assumes that a single meteorite impact led to a sunlight-blocking atmospheric dust plume that severely affected photosynthesis and reduced global temperature, leading to an "impact winter". Their hypothesis rests on anomalous amounts (3 $ng \cdot g^{-1}$) of iridium, an element abundant in meteorites but rare in terrestrial crustal rocks, in a 1-centimeter-thick clay layer within a sequence of pelagic limestones at Gubbio (Italy). Subsequently, an increasing number of observations seem to support a meteorite impact at the KTB: (a) iridium anomalies detected at almost one hundred sites, homogeneously distributed worldwide (Claeys et al., 2002), (b) presence of glass microspherules (Smit and Klaver, 1981; Smit, 1999) (c) finding of shocked quartz (Bohor et al., 1984; Bohor, 1990; Morgan et al., 2006; Kamo et al., 2011) and (d) discovery of the large Chicxulub crater in the Yucatán Peninsula (Swisher et al., 1992) in Mexico, claimed as the site for the large bolide impact invoked by Alvarez et al. (1980).

Stüben et al. (2005) reported a high-resolution geochemical data of eight KTB sequences in Mexico, considered critical in the reconstruction of the nature of the KTB events and their environmental consequences. Their study has revealed less pronounced, but still significant, Ir anomalies (0.2–0.8 $ng \cdot g^{-1}$) in most of the investigated KTB sections, and a complex depositional history across the Chicxulub impact site and KTB events. Stüben et al. (2005) concluded that the Ir anomalies originated from an impact event and that these anomalies are stratigraphically and geochemically decoupled from the underlying spherule-rich ejecta deposit related to the Chicxulub event. These findings suggest two or more impact events, separated by a considerable amount of time. Stüben et al. (2005) also reported the presence of bentonite layers and Pt and Pd-dominated PGE anomalies below and above the KTB as an indication of volcanic activity. They have shown that C and O-isotope patterns for these sections indicate a gradual climatic change during the latest Maastrichtian, an abrupt change at the KTB, and a slight recovery during the lowermost Paleocene.

In contrast with these above-mentioned conclusions, Denne et al. (2013) have reported a KTB massive deposit in deep-water Gulf of Mexico which substantiates widespread slope failure induced by the Chicxulub impact and that provides further evidence of a single impact coincident with the KTB mass extinction.

The hypotheses of one or multiple meteorite impacts as the main cause of mass extinction during the KTB, however, have never reached a consensus. It is known that the largest mass extinction in the Earth's history, the Permian–Triassic boundary (PTB), coincides in time with basaltic flows in Siberia (Campbell et al., 1992; Renne et al., 1995; Berner, 2002; Beerling et al., 2007; Sanei et al., 2012). Likewise, it is feasible to suggest/assume that the perturbation in the carbon cycle and the iridium anomalies in the KTB resulted from volcanism of a magnitude equivalent to that of the Deccan traps of west-central India, whose gigantic eruptions produced huge volumes of flood basalt (up to 2 km in thickness) between 68 and 60 million years ago (Sheth, 2005). The discovery of rapid and voluminous Deccan basalt eruptions at the KTB led to the hypothesis that part of the iridium and other PGE concentrations in KTB sections may well be attributable directly to a volcanic origin rather than to a meteoritic one.

It has been hypothesized that anomalous Hg levels caused by catastrophic Siberian Trap volcanic eruptions were associated with the mass extinction of the Permian–Triassic boundary (Sanei et al., 2012), informally known as the "Great Dying" (Morrison, 2004). An asteroid impact as an alternative explanation for PTB mass extinction (e.g., Becker et al., 2001 and references therein) has never assembled as much evidence as for the KTB although a meteor crater dated at 250.7 $\pm$ 4.3 million years (argon–argon date from a single plagioclase crystal; Morrison, 2004) was identified near the coast of Australia.

Courtillot and Renne (2003) and Wignall (2001) believed that the onset of a large igneous province (LIP) eruption often postdated the mass extinction and that only the eruption of the Deccan Traps coincided precisely with a mass extinction. The Deccan eruptions may have transferred to the atmosphere an enormous amount of metals, including Hg, worsening the environmental conditions and leading to the huge KTB mass extinction, in a similar way to that proposed for the Siberian Traps that emitted $3.8 \times 10^9$ tons of Hg (Sanei et al., 2012).

In South America, sedimentary sequences that encompass the KTB are found in the Salta (Balbuena Subgroup) and Neuquén basins, Argentina (Marquillas and Salfity, 1988; Salfity and Marquillas, 1994; Sial et al., 2001; Marquillas et al., 2003, 2005; Scasso et al., 2005; Aberhan et al., 2007; Keller et al., 2007; Marquillas et al., 2007, 2011), and in the Paraíba Basin, northeastern Brazil (Sial et al., 2001; Neumann et al., 2009; Nascimento-Silva et al., 2011). Sedimentary sequences that potentially record the KTB are found in Navidad (Topocalma Point) and Magellan basins (Punta Arenas) in Chile (Sial et al., 2001).

### 2.1. The studied sections

In this study, we address the Hg chemostratigraphy at the Paraíba and Salta basins, where the KTB has been studied in sufficient detail. These studies did not result in a positive identification of meteoritic impact ejecta influence in the sedimentary logs, but an association of the KTB sedimentary rocks with volcanic ash beds was described by Marquillas et al. (2011). Besides, we also look at the Hg behavior across the KTB at Stevns Klint, a classical locality in which evidence

for meteorite impact has been substantially documented (Frei and Frei, 2002, and references therein).

*2.1.1. The Salta Basin, Northwestern Argentina*

The Balbuena Subgroup (Upper Campanian–Danian) represents the sedimentary infill of the initial post-rift stage of the Salta Basin (Lower Cretaceous–Eocene), NW Argentina, with an average thickness of 450 m. It comprises three lithostratigraphic units, from the base to the top: Lecho (white aeolian sandstones), Yacoraite (shallow marine limestones) and Olmedo (dark lacustrine shales) formations (Salfity and Marquillas, 1994; Marquillas et al., 2005). The Yacoraite limestone is the most conspicuous stratigraphic unit in the Balbuena Subgroup with several members (Amblayo, Guemes, Alemanía and Juramento).

An attempt to locate the position of the KTB in the Balbuena Subgroup using carbon isotopes, besides other information, was made by Sial et al. (2001) and Marquillas et al. (2003, 2007). The study by the former authors pointed to the contact between the Yacoraite and Olmedo formations as the locality of the KTB, based on a marked negative $\delta^{13}C$ excursion (around −5‰) (Fig. 1).

Some consolidated volcanic tuffs from the Yacoraite Formation, with outcrops exposed at the Cabra Corral Dam and Juramento River, have been dated (Marquillas et al., 2011). Almost all known levels of volcanic ash tuffs in the Yacoraite Formation are intercalated in its lower part (Amblayo Member), where at least five volcanic tuff levels, with an average thickness of 25 cm, are observed. One single tuff level also occurs in the upper middle part of the column (Alemanía Member; Marquillas et al., 2011). U–Pb zircon age determination of two of these volcanic tuff layers (Marquillas et al., 2011), by LA-MC-ICP-MS, yielded ages of 71.9 ± 0.4 Ma (base of the Amblayo Member) and 68.4 ± 0.7 Ma (Alemanía Member; indicated in Fig. 2a). This information suggests that the KTB is located above the Alemania Member and supports the position pointed by Sial et al. (2001).

The crystallization age of some of the volcanic tuffs intercalated with the Olmedo Formation above the Yacoraite Formation have been recently investigated using the zircon LA-ICPMS method by Pimentel et al. (2012). The basal tuff at the contact of the Yacoraite and Olmedo formations investigated by these authors yielded an age of 64.90 ± 0.87 Ma and is interpreted as the best estimate for its crystallization age. One additional volcanic tuff sample, interlayered with black shales in the upper part of the Olmedo Formation, indicated and age of 60.3 ± 2.1 Ma.

In summary, the age determinations of the volcanic tuffs interlayered with the Yacoraite and the Olmedo formations confirm that the KTB is located at the contact between the Yacoraite and Olmedo formations.

*2.1.2. The Paraíba Basin, northeastern Brazil*

The KTB in the Paraíba Basin, northeastern Brazil is observed in a carbonate sequence represented by the Maastrichtian Gramame and the Danian Maria Farinha formations (Fig. 3). The coastal portion of this basin occupies an area of about 7600 $km^2$ and its offshore area is about 31,400 $km^2$, extending into the continental shelf and down to 3000 m depth.

The Paraíba Basin shows a preserved succession of almost continuous sediment deposition across the KTB. Despite an important sea-level fall during the early Paleocene that has affected the critical layer of this transition which is associated with the P0 biozone, it is observed that continuous deposition characterized this KTB section (Stinnesbeck and Keller, 1996; Morgan et al., 2006; Neumann et al., 2009; Gertsch et al., 2013). This event caused erosion that has affected most of the basin and caused reworking of lower Danian and uppermost upper Maastrichtian deposits (Stinnesbeck and Keller, 1996; Neumann et al., 2009). In consequence, the KTB is marked by a conglomeratic carbonate layer formed by deposits from both stages.

Carbon and oxygen isotope chemostratigraphy from the drill cores at the Poty quarry, Itamaracá and Olinda localities at the Olinda Sub-basin was studied by Nascimento-Silva et al. (2011) and will be discussed below.

*2.1.3. Danish Basin, Stevns Klint, Denmark*

Stevns Klint, a classical KTB locality, is a 14.5 km long coastal cliff south of Copenhagen, Denmark (Fig. 4), and the type locality of the Danian stage together with the nearby Faxe quarry. Perhaps the two most detailed stratigraphic studies of this area are those accomplished by Surlyk et al. (2006) and Lauridsen et al. (2012). The KTB at this place is famous for its large Ir anomaly of about 160 times the background (Alvarez et al., 1980; Hansen et al., 1988; Schmitz et al., 1988), which is taken as evidence of extraterrestrial components. It has been often used as one of the examples where there are several lines of evidence in favor of the asteroid impact theory.

Relatively high concentrations of elements like Ni, Co, and Zn, besides Ir, observed at many KTB localities worldwide, are found enriched in the boundary layer at Stevns Klint (Christensen et al., 1973; Schmitz, 1985; Elliott, 1993). Frei and Frei (2002) have conducted a multi-isotopic and trace element investigation of the Cretaceous–Paleogene boundary layer at this locality, aiming to contribute to the question regarding the nature or type of the KTB impactor by applying Os isotopes and lithophile element fingerprinting. Os, Sr, Nd and Pb isotope data were obtained from a profile across the KTB layer (Fiskeler Member, informally known as Fish Clay, about 5 to 10 cm thick, separating the underlying Maastrichtian chalk from the overlying Danian limestone sequence; Fig. 2c). The behavior of these isotopes in the Fish Clay layer at the KTB, according to Frei and Frei (2002), supports that PGEs originated from global input of cosmogenic material into the ocean derived from a likely chondritic impactor.

High resolution C- and O-isotope investigations at the Stevns Klint succession across the KTB were performed by Hart et al. (2004) and Machalski and Heinberg (2005). Hart et al. (2004) and Machalski and Heinberg (2005) found a $\delta^{13}C$ negative excursion at the KTB (values drop from around +2‰ in the uppermost Højerup Member to +1‰ at the Fiskeler Member), while chemostratigraphic curve shows a negative $\delta^{18}O$ anomaly (around −1.5‰ V-PDB).

## 3. Analytical methods

Homogenized 0.5 to 1.0 g samples of sediments, dried at 60 °C to constant weight, were digested with an acid mixture (50% *aqua regia* solution), and heated at 70 °C for 1 h, in a thermal-kinetic reactor ("cold finger"). Glass and plasticware were decontaminated by immersion for 2 days in 10% (v/v) Extran solution (MERCK), followed by immersion for 3 days in diluted $HNO_3$ (10% v/v) and final rinsing with Milli-Q water. All chemical reagents used were of at least analytical grade. Cold Vapor Atomic Fluorescence Spectrophotometry, using a Millennium PSA2 AFS spectrophotometer, was used for Hg determination, after $Hg^{2+}$ reduction with $SnCl_2$. All samples were analyzed in duplicates, showing reproducibility within 9.5%. A certified reference material (NRC PACS-2, Canada) was simultaneously analyzed to evaluate Hg determination accuracy. Such analysis showed a precision of 4%, as indicated by the relative standard deviation of three replicates, and presented Hg recovery of 98.8 ± 6.2%. The Hg detection limit estimated as 3 times the standard deviation of reagent blanks, was 1.26 $ng \cdot g^{-1}$. In all cases, blank signals were lower than 0.5% of sample analysis. Concentration values were not corrected for the recoveries found in the certified material.

As for the thermo-desorption analyses, about 100 to 300 mg from dried selected samples of the Yacoraite Formation were heated, in triplicate, in a DMA Hg analyser in a sequence of programmed temperatures: 50, 100, 150, 200, 250, 300, 400 e 500 °C. In these experiments, 1.5 min was taken to reach each cited temperature and 2 min spent in heating at each temperature. Commercial oxygen was used as carrier gas in a flow rate of 200 mL/min.

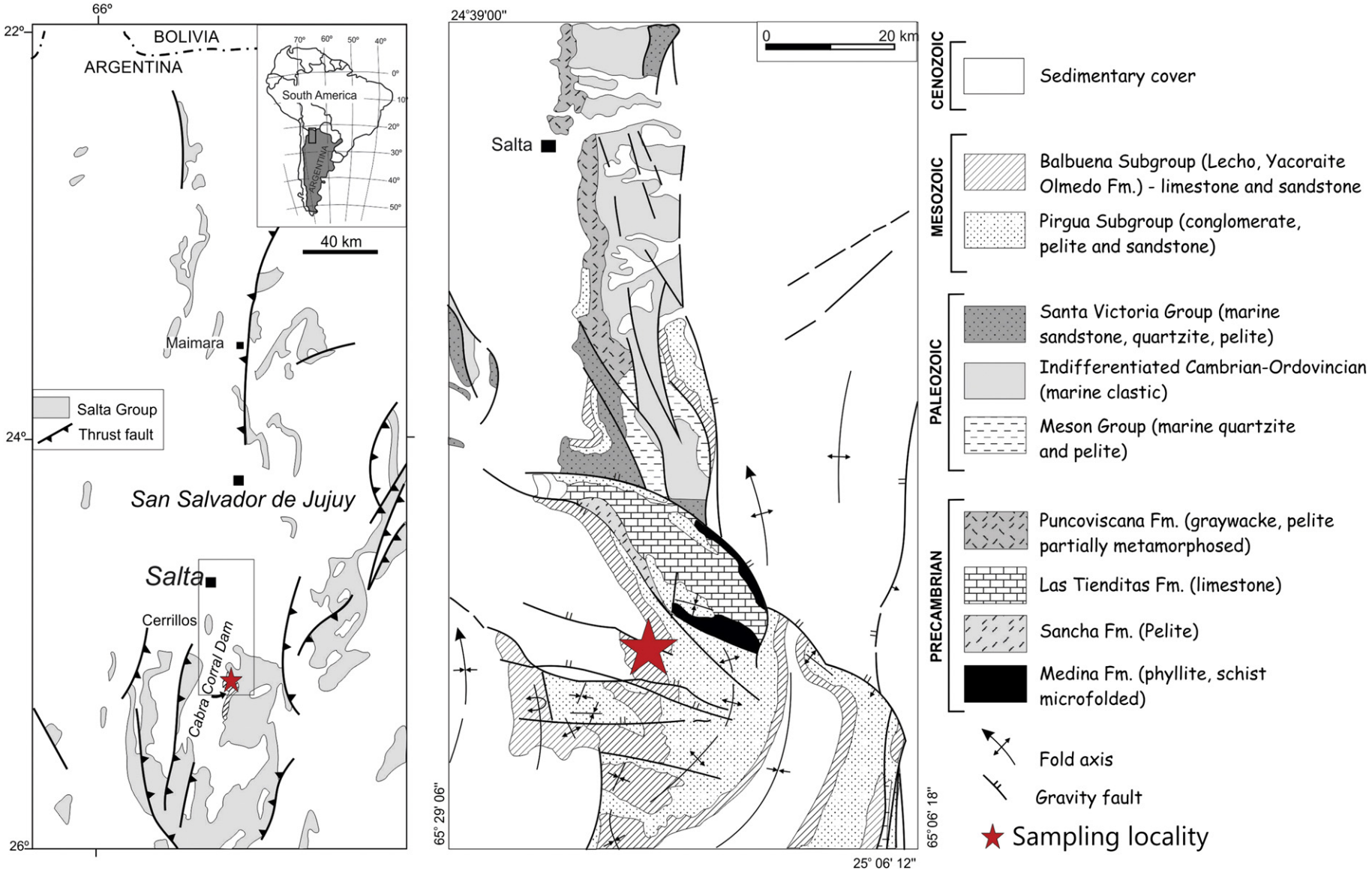


**Fig. 1.** (a) Sites of occurrence of the Yacoraite Formation in Jujuy and Salta provinces, Argentina, including the Maimara and Cabra Corral localities; (b) geologic map of the Cabra Corral area, about 70 km south of Salta. After Salfity et al. (1998).


**Fig. 2.** (a) Section of the Yacoraite Formation across the KTB (Güemes Member to the left and Alemanía, to the right), Provincial road n. 47, Cabra Corral, Salta Province, Argentina. Arrow indicates the location of a volcanic ash tuff. The KTB was supposed to be midway between the roof of the red bank (extreme left) and the contact with the Alemanía Member to the right (Marquillas et al., 2007). The U–Pb age of this volcanic tuff (68 Ma) constrains the KTB, however, to a position stratigraphically above it (Marquillas et al., 2011); (b) KTB at the Poty quarry, Olinda sub-basin, northeastern Brazil; (c) view of the sampled section at Stevns Klint, Denmark (Fig. 7).

Analyses of C and O isotopes of carbonates were performed at the Stable Isotope Laboratory (LABISE) of the Department of Geology, Federal University of Pernambuco, Brazil. Extraction of $CO_2$ gas from microdrilled powder (1 mm drill bit was used, avoiding fractures, recrystallized portions and weathered surfaces) was performed in a high vacuum line after reaction with 100% orthophosphoric acid at 25 °C for one day (three days allowed, when dolomite was present). Released $CO_2$ was analyzed after cryogenic cleaning in an Isotech double inlet, triple-collector SIRA II or Thermofinnigan Delta V Advantage mass spectrometers and results are reported in δ notation in permil (‰) relative to the VPDB standard. The uncertainties of the isotope measurements were better than 0.1‰ for carbon and 0.2‰ for oxygen, based on multiple analyses of an internal laboratory standard (BSC). Alumina oxide analyses were performed on bulk samples by X-ray fluorescence at the LABISE, using a Rigaku RIX 3000 XRF unit equipped with a Rh tube.

## 4. Mercury behavior across the KTB

Mercury concentrations measured in ten samples across the KTB in the Balbuena Subgroup, in Argentina, in a section next to a bridge in the Provincial road N. 47 (Fig. 2; same section studied by Sial et al., 2001), revealed four spikes. One of them presents about 20 $ng \cdot g^{-1}$ Hg (Table 1) and coincides with the transition between the Yacoraite and Olmedo formations (Fig. 5a). This spike immediately predates minimum $\delta^{13}C$ (around −5‰) and $\delta^{18}O$ values (around −10‰ VPDB).

Mercury concentration has also been analyzed in twenty-five samples across the middle and upper part of the Yacoraite Formation (Guemes and Alemanía members), collected in a section about 80 m thick in the Provincial road N. 47 (Table 1). At this place, the Yacoraite Formation reaches about 200 m in thickness. Results have been plotted along $Al_2O_3$ (data from Marquillas et al., 2007) and $\delta^{13}C$ and $\delta^{18}O$ chemostratigraphic curves with 60 samples collected in the same stratigraphic interval, in the present study (Fig. 5b). The Hg chemostratigraphic curve revealed about five spikes, the largest one with about 250 $ng \cdot g^{-1}$ (labeled IV in Fig. 5b), is above a 68 Ma ash bed and below the transition to the Olmedo Formation which displays a smaller Hg spike (labeled V in Fig. 5b), a $\delta^{13}C$ excursion of about −3‰ and that corresponds to the KTB.

The negative $\delta^{13}C$ excursion of about −3‰ likely corresponds to a sea-level fall just before the KTB observed in several places in the world as mentioned by Alvarez et al. (1980).

The Hg concentrations in samples across the KTB in three drill cores of the Paraíba Basin (Itamaracá, Olinda and Poty drill holes; Table 1) display less pronounced spikes if compared to those of the Yacoraite Formation in Argentina. As these samples are from drill holes, Hg concentrations are likely devoid of anthropogenic contamination.

In the Itamaracá drill core (Fig. 6a), the main Hg spike in ten samples appears immediately above the supposed location of the KTB. There is a clear co-variation of Hg with alumina; the $\delta^{13}C$ stratigraphic variation curve does not show the pronounced negative excursion before the KTB as recorded in Argentina and in several other KTB localities worldwide. In the Olinda drill core (Fig. 6b), ten samples display a 12 $ng \cdot g^{-1}$ Hg spike at less than 1 m below the supposed location of the KTB. The Hg content decreases towards this transition as it does the alumina content. Above the transition, the Hg curve exhibits a discrete spike. In the Poty drill hole (Fig. 6c), Hg concentration has been analyzed in twenty-two samples. Hg contents from the Maastrichtian Gramame Formation display very discrete Hg peaks and a spike (3 $ng \cdot g^{-1}$) above the supposed location of the KTB. The alumina and the Hg stratigraphic variation curves roughly display co-variation. In addition, the $\delta^{13}C$ stratigraphic variation curve displays four negative excursions towards the top of the Gramame Formation, but no corresponding excursion in the $\delta^{18}O$ stratigraphic variation curve is seen. Only very discrete to absent Hg spikes correspond to these $\delta^{13}C$ negative excursions.

In all these three drill holes, an increase in $\delta^{18}O$ right above the KTB, if near-primary signal, suggests a temperature decrease, something also observed in the two profiles studied in the Yacoraite–Olmedo transition in Argentina.

Results of Hg concentrations in eight samples from across the KTB at the same Stevns Klint locality analyzed for Sr, Nd, Pb and Os isotopes by Frei and Frei (2002) are listed in Table 1. In Fig. 7, the Hg stratigraphic variation curve has been plotted along $Al_2O_3$ (data are from Schmitz et al., 1992), $^{87}Sr/^{86}Sr$, $^{206}Pb/^{204}Pb$ (t = 65 Ma) and $^{187}Os/^{188}Os$ (t = 65 Ma) from (Frei and Frei, 2002) stratigraphic variation curves. A peak of Hg of about 260 $ng \cdot g^{-1}$ in the Fish Clay layer at the KTB displays a clear correlation with a $^{87}Sr/^{86}Sr$ peak that, in turn, witnesses an increase of continental weathering, subsequent clay generation and Hg fixation.

## 5. Discussion and conclusions

Volcanic emissions are a significant natural source of Hg to the atmosphere with average annual emissions of about 90 tons, 60% of which are from eruptions and 40% from degassing activities (Nriagu and Becker, 2003). Volcanic eruptions increase atmospheric Hg concentration and subsequently Hg atmospheric deposition. However, deposition is also enhanced by the increased formation of soluble Hg compounds in atmospheric water droplets, more acidic due to

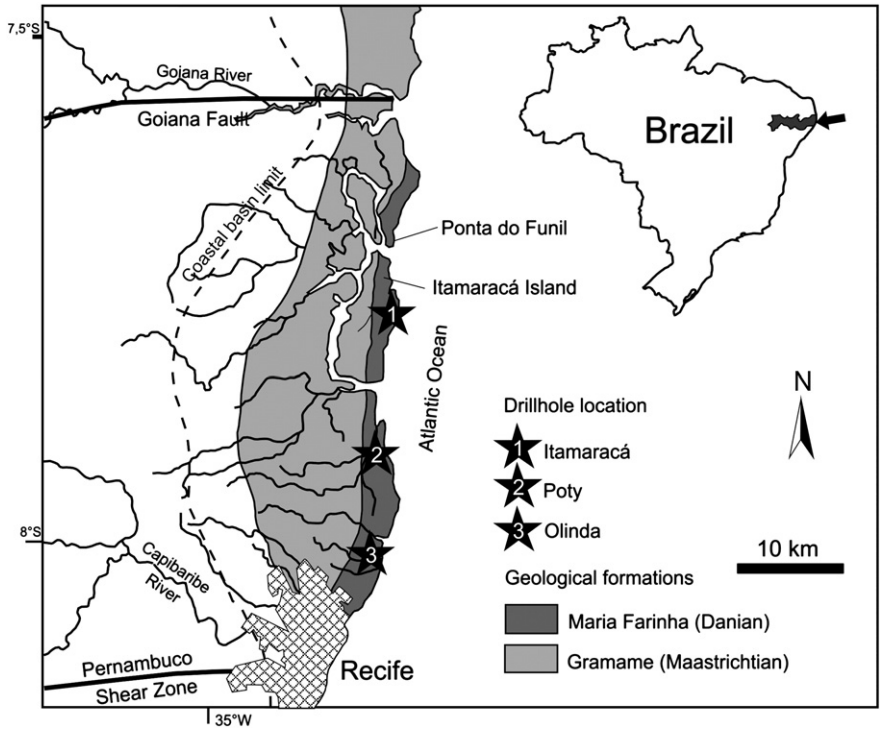


**Fig. 3.** Map of the Paraíba Basin, location of its three sub-basins and of the three studied drill holes: Poty quarry, Olinda and Itamaracá.

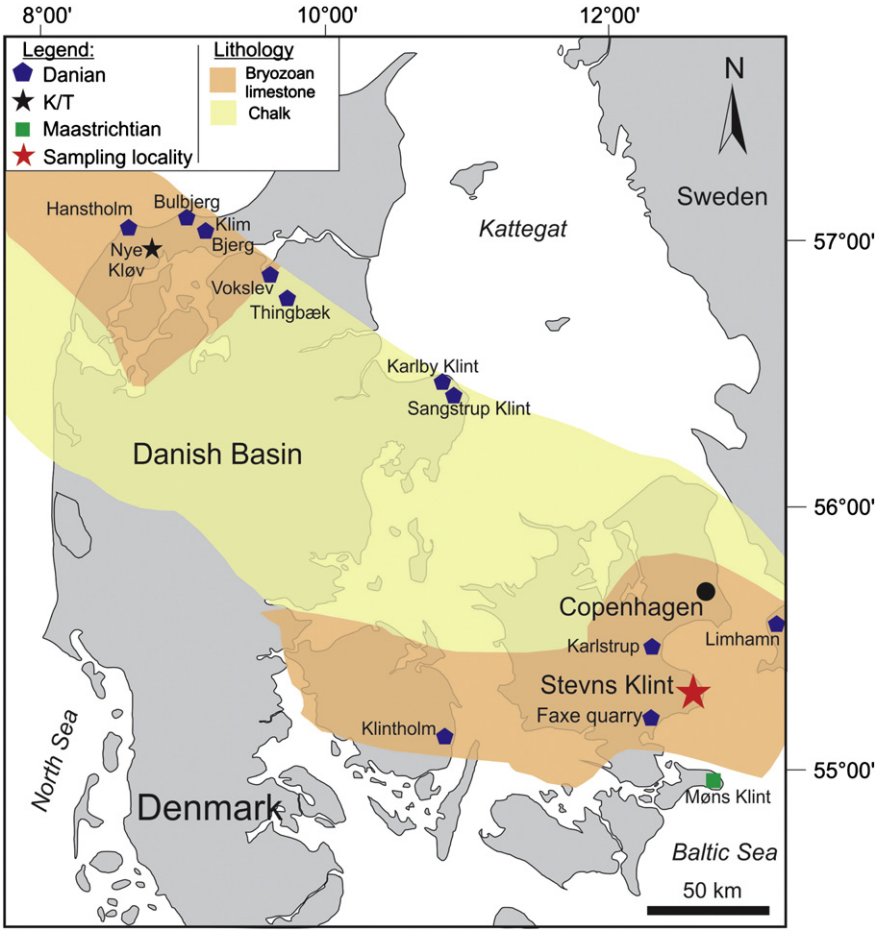


**Fig. 4.** Map of Denmark with major structural elements showing location of sampled site at Stevns Klint. Modified from Surlyk et al. (2006) and Lauridsen et al. (2012).

**Table 1**
Mercury contents ($ng \cdot g^{-1}$) for Cretaceous–Paleogene bulk samples from Brazil, Argentina and Denmark.

| Cretaceous–Paleogene transition (KTB) Carbonates | | | |
|---|---|---|---|
| Northeastern Brazil | | | |
| Formation | Sample | Height (cm) | Hg |
| (a) Itamaracá drill hole, Paraiba Basin | | | |
| Maria Farinha | D 3240 | 32.4 | 2.91 |
| | D 3270 | 32.7 | 2.97 |
| | D 3300 | 33 | 3.35 |
| | D 3360 | 33.6 | 4.38 |
| | D 3390 | 33.9 | 3.85 |
| Gramame | D 3420 | 34.2 | 1.59 |
| | D 3450 | 34.5 | 1.06 |
| | D 3480 | 34.8 | 0.84 |
| | D 3510 | 35.1 | 2.6 |
| | D 3540 | 35.4 | 1.5 |
| (b) Olinda drill hole, Paraiba Basin | | | |
| Maria Farinha | D 3630 | 36.3 | 2.1 |
| | D 3660 | 36.6 | 1.2 |
| | D 3690 | 36.9 | 2.3 |
| | D 3720 | 37.2 | 2.2 |
| | D 3750 | 37.5 | 2.2 |
| | D 3810 | 38.1 | 1.7 |
| | D 3840 | 38.4 | 4.5 |
| Gramame | D 3900 | 39 | 2.3 |
| | D 3960 | 39.6 | 8.9 |
| | D3990 | 39.90 | 11.5 |
| (c) Poty drill hole, Paraiba Basin | | | |
| Maria Farinha | D 114 | 11.4 | 1.37 |
| | D 117 | 11.7 | 2.64 |
| | D 123 | 12.3 | 0.39 |
| Gramame | D 126 | 12.6 | 0.73 |
| | D 129 | 12.9 | 0.14 |
| | D 132 | 13.2 | 0.13 |
| | D 135 | 13.5 | 0.5 |
| | D 138 | 13.8 | 0.53 |
| | D 141 | 14.1 | 0.18 |
| | D 144 | 14.4 | 0.46 |
| | D 171 | 17.1 | 0.16 |
| | D 174 | 17.4 | 0.27 |
| | D 177 | 17.7 | 0.42 |
| | D 201 | 20.1 | 0.12 |
| | D204 | 20.4 | 0.28 |
| | D207 | 20.7 | 0.25 |
| | D222 | 22.2 | 0.43 |
| | D225 | 22.5 | 0.17 |
| | D228 | 22.8 | 0.38 |
| | D276 | 27.6 | 0.48 |
| | D279 | 27.9 | 0.56 |
| | D282 | 28.2 | 0.46 |
| (d) Poty quarry section, Paraiba Basin | | | |
| Maria Farinha | 1-PO-01-PE 9,32 | 0 | 8.2 |
| | 1-PO-01-PE 9,45 | 0.13 | 11.6 |
| | 1-PO-01-PE 9,5 | 0.18 | 11.4 |
| | 1-PO-02-PE 9,6 | 0.28 | 14.3 |
| | 1-PO-01-PE 10,05 | 0.73 | 11.2 |
| | 1-PO-01-PE 10,12 | 0.8 | 10.5 |
| | 1-PO-01-PE 11,7 | 2.38 | 10.5 |
| | 1-PO-01-PE 12,55 | 3.23 | 9.5 |
| | 1-PO-01-PE 13,2 | 3.88 | 16.6 |
| Gramame | 1-PO-01-PE 14,75 | 5.43 | 9.4 |
| | 1-PO-01-PE 14,85 | 5.53 | 13.0 |
| | 1-PO-01-PE 15,2 | 5.88 | 6.3 |
| | 1-PO-01-PE 17,32 | 8.0 | 8.0 |
| Cretaceous–Paleogene transition (KTB) bulk samples | | | |
| Argentina | | | |
| Formation/Member | Sample | Height (cm) | Hg |
| (e) Yacoraite Formation, Cabra Corral, Provincial road N. 47 | | | |
| Maastrichtian Yacoraite Formation (Alemanía Member) | E-37 | 0 | 7.41 |
| | E-36 (all) | 80 | 34.52 |
| | E-34 | 150 | 4.07 |
| | E-31 | 360 | 1.54 |

**Table 1** (*continued*)

| Cretaceous–Paleogene transition (KTB) bulk samples | | | |
|---|---|---|---|
| Argentina | | | |
| Formation/Member | Sample | Height (cm) | Hg |
| (e) Yacoraite Formation, Cabra Corral, Provincial road N. 47 | | | |
| Maastrichtian Yacoraite Formation (Alemanía Member) | E-30 | 610 | 13.93 |
| | E-29 | 570 | 6.06 |
| | E-28 | 180 | 75.22 |
| | E-27 | 180 | 75.22 |
| | C-908 | 15 | 248.23 |
| | E-26 | 520 | 6.92 |
| | E-25 | 40 | 7.39 |
| | E-24 | 75 | 5.65 |
| | E-23 | 170 | 12.38 |
| | C-604 | 1100 | 139.97 |
| | C-602 | 80 | 147.97 |
| | C-405 | 2130 | 12.28 |
| | C-319 | 370 | 199.64 |
| | C-318 | 60 | 70.85 |
| Maastrichtian Yacoraite Formation (Güemes Member) | C-315 | 540 | 3 |
| | C-313 | 225 | 39.6 |
| | C-108 | 420 | 35.3 |
| | K-14-E | 170 | 18.64 |
| | K-G | 190 | 12.42 |
| Maastrichtian Yacoraite Fm. (Amblayo Member) | K-I | 180 | 7.44 |
| | K-J | 190 | 8.36 |
| | K-14-K | 90 | 38.61 |
| (f) Yacoraite and Olmedo formations, Cabra Corral Dam, by the bridge | | | |
| Danian Olmedo Formation | Yacor-24 | 40.1 | 10.4 |
| | Yacor 23 | 23.5 | 3.66 |
| | Yacor 17 | 2.65 | 1.51 |
| | Yacor 16 | 14.85 | 1.51 |
| Maastrichtian Yacoraite Formation (Alemanía Member) | Yacor-12 | 6.5 | 19.07 |
| | Yacor-11 | 5.3 | 9.8 |
| | Yacor-9 | 29.1 | 14.26 |
| | Yacor-5 | 14.15 | 1.51 |
| | Yacor-3 | 11.8 | 18.66 |
| | Yacor-1 | 0 | 12.87 |
| Denmark | | | |
| Formation/member | Sample | Height (cm) | Hg |
| (g) Stevns Klint (Højerup) | | | |
| Danian Stevns Klint Formation | D3 | 30 | 4.55 |
| | D2 | 15 | 4.51 |
| Danian Rødvig Formation (Fiskeler Member; KTB) | FC-1 | Bulk | 127.72 |
| | FCD | 3 | 67.9 |
| | FCC | 2 | 257.94 |
| | FCB | 1 | 194.53 |
| | FCA | 0 | 108.76 |
| Maastrichtian Tor Formation (Højerup Member) | M2 | −15 | 9.09 |
| | M1A | −30 | 0.88 |

the simultaneous emission of volcanic gases (Roos-Barraclough et al., 2002). Gaseous Hg from volcanic activity are transported far from source reaching a regional and even global scale, contrary to most elements present in ash. As a result, many studies have reported synchronous Hg spikes in the sedimentary record associated with recent (e.g. Martínez-Cortizas et al., 1999; Roos-Barraclough et al., 2002; Roos-Barraclough and Shotyk, 2003) and prehistoric volcanic activity (e.g. Sial et al., 2010; Nascimento-Silva et al., 2011; Sanei et al., 2012).

Maastrichtian limestone and Danian marl and limestone samples from across the Yacoraite KTB were submitted to thermo-desorption sequence and less than 3% of total Hg content was released under 100 °C. The major proportion of the Hg content (~75%) was released between 200 °C and 250 °C (Fig. 8), characterizing $Hg^{2+}$ as the major Hg species present (Valle et al., 2005), supporting volcanogenic origin followed by transport and oxidation under acidic conditions, in agreement with regional to global distribution and increased atmospheric deposition. Typical releases observed in meteorites at the 200 °C and 250 °C temperature range is about 40% of the total Hg content only,

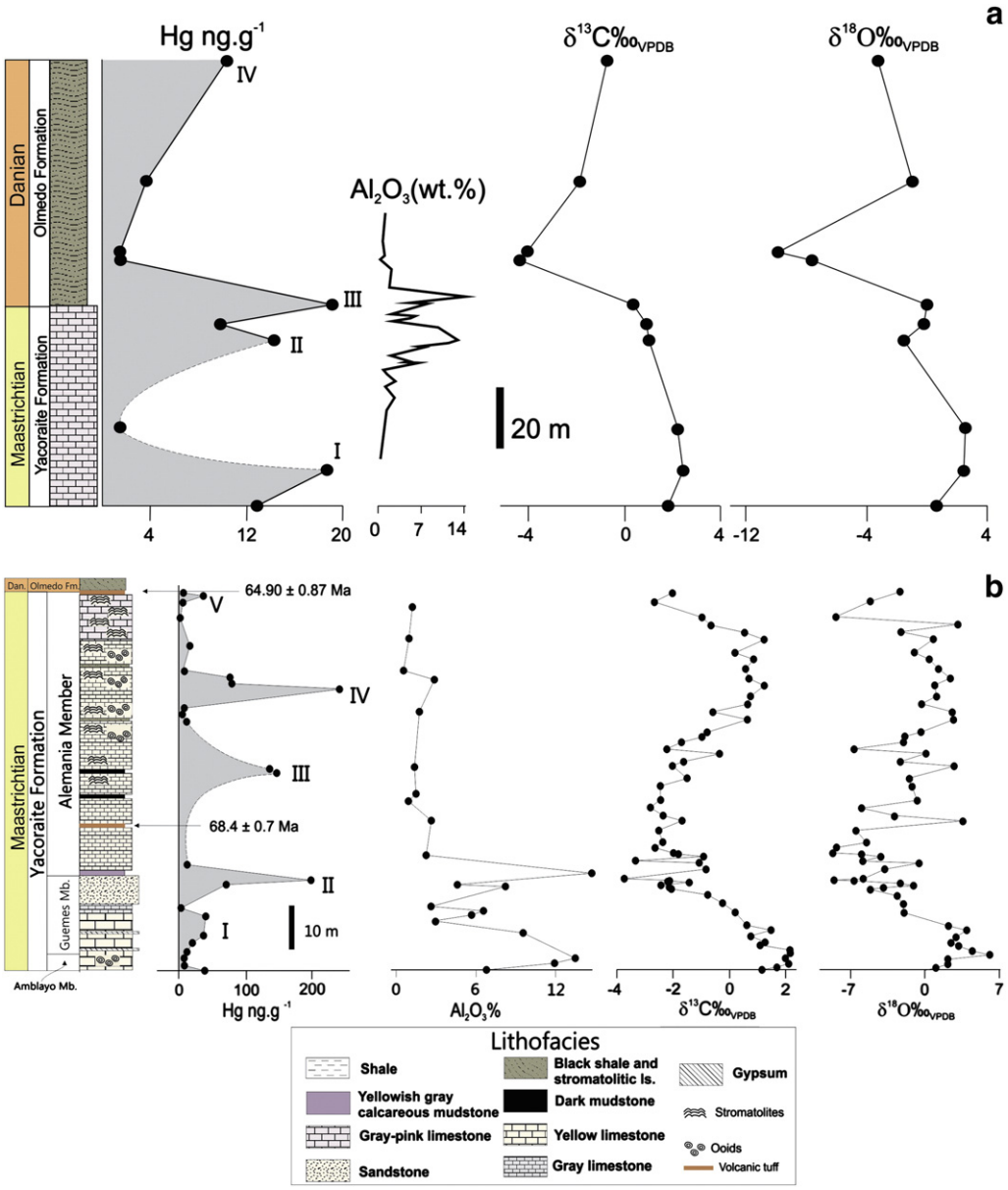


**Fig. 5.** Hg, $Al_2O_3$, $\delta^{13}C$ and $\delta^{18}O$ stratigraphic variation curves across the KTB, Yacoraite–Olmedo formations, Cabral Corral: (a) profile next to the bridge; (b) Provincial road n. 47; $Al_2O_3$ curve is from Marquillas et al. (2007); approximate stratigraphically locations of volcanic tuffs dated with 68.4 ± 0 (within Yacoraite Formation; Marquillas et al., 2011) and 64.90 ± 0.87 Ma (within Olmedo Formation; Pimentel et al., 2012) are indicated.

with a similar fraction released in temperatures lower than 100 °C (Kumar et al., 2001). When reaching a surface environment that is depleted of organic scavenging capacity due to climate changes at the KTB, $Hg^{+2}$ would be kept mostly in solution, readily adsorbed onto clays and transported to sedimentary basins. In summary, high levels of Hg associated to clay-bearing carbonates is in agreement with an increased flux of volcanic-derived Hg from the landmass into the marine realm.

Anomalous Hg contents have been observed below and above the transition of the Maastrichtian to Danian in Dolenja Vas (Palinkaš et al., 1996) in southwestern Slovenia, and have been regarded as a probable result of subaerial volcanic activity during this transition. Anomalies in Hg contents across the KTB have been also observed by Hildebrand and Boynton (1989) who have claimed this as evidence for the acid rain they have deemed responsible for the mass extinction at the KTB. In addition, anomalous Hg levels from catastrophic Siberian Traps volcanic eruptions have been associated with the latest Permian extinction on northwest Pangea (Sanei et al., 2012).

Anomalous amounts of Hg are recorded below and above the KTB in the Paraíba Basin, similar to peaks observed in Dolenja Vas. The highest Hg values (almost 250–260 $ng \cdot g^{-1}$) encountered at Yacoraite are comparable to those observed in Stevns Klint. In the Yacoraite Basin, no evidence for a meteorite impact has been mentioned. Volcanic activity across the KTB, instead, is indicated by the presence of volcanic tuffs. Therefore, it is possible that high Hg levels observed are tied to volcanic activity.

A complication for the origin of Hg, particularly in KTB sections, arises from the fact that meteorites may carry large amounts of Hg. Ozerova et al. (1973) reported an average of 6 $ng \cdot g^{-1}$ Hg in stone meteorites (abundance from 0 to 33 $ng \cdot g^{-1}$), about 500 $ng \cdot g^{-1}$ in carbonaceous chondrites, iron meteorites displaying the lowest Hg concentrations (generally <0.1 $ng \cdot g^{-1}$). Lauretta et al. (2001) have reported bulk abundances of Hg of 294 ± 15 and 30 ± 1.5 $ng \cdot g^{-1}$ for the Murchison and Allende carbonaceous chondrites, respectively. In addition, Shima et al. (1974) have reported a bulk Hg analysis of 1330 $ng \cdot g^{-1}$ for the Parambu chondrite (state of Ceará, Brazil).

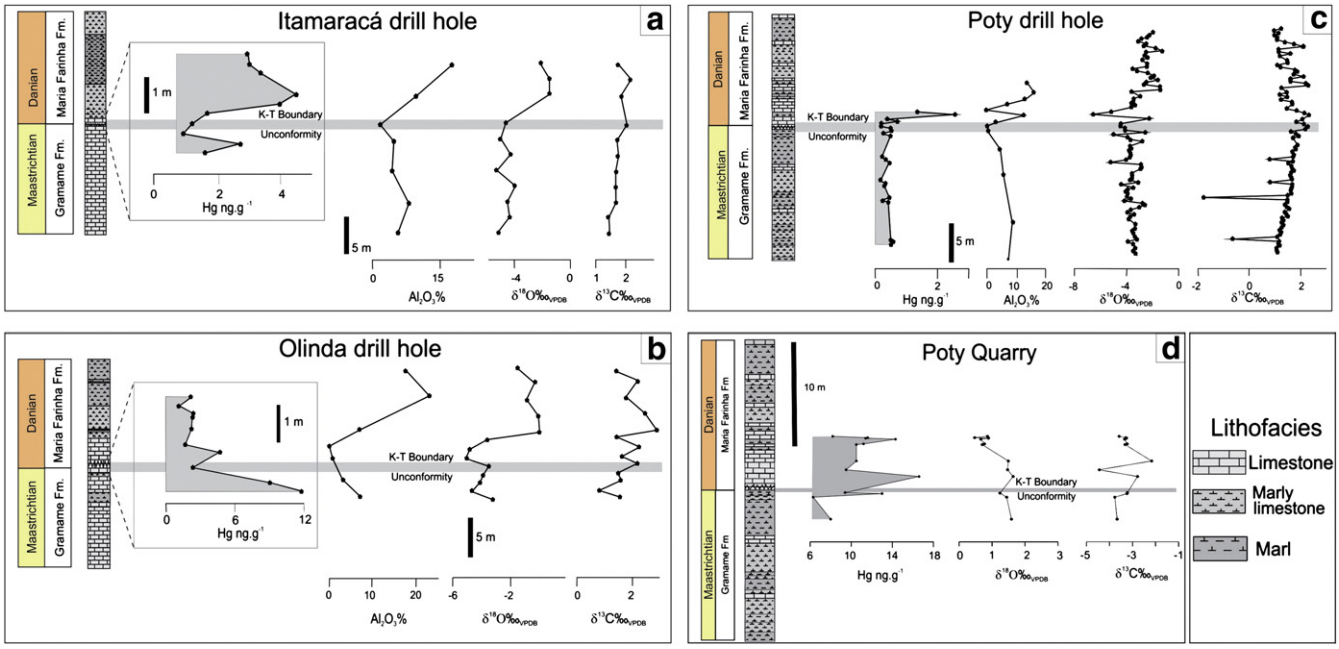


**Fig. 6.** Hg, $Al_2O_3$, $\delta^{13}C$ and $\delta^{18}O$ stratigraphic variation curves across the KTB in three drill cores, Paraíba Basin, northeastern Brazil.

The nature of the main meteorite impactor is under debate but short-lived Cr isotopic compositions of sedimentary rocks from the KTB, for some authors, point to a Hg-poor carbonaceous chondrite-type bolide (e.g. Shukolyukov and Lugmair, 1998). Also, most of these studies, with the exception of Lauretta et al. (2001), have used analytical methodologies which are not advised for Hg analysis (see for example Randa et al., 2003). Analysis of samples from the Allende chondrite reviewed by Lauretta et al. (2001), for example, gave values ranging from 16.4 to 10,020 $ng \cdot g^{-1}$, whereas the same meteorite analyzed by Kumar et al. (2001) gave much smaller concentrations of 16.4 to 17.8 $ng \cdot g^{-1}$. One reason for the large variability of Hg content in meteorites, so far reported, is due to erroneous determination of Hg, mostly by radiochemical neutron activation, that ignored the presence of $^{75}Se$ in the released Hg fraction, resulting in an overestimation of the Hg content (Kumar et al., 2001). Bulk Hg analysis may also blur the actual Hg content due to contamination. As for example, sequential thermo-desorption has been applied to a sample of the Antarctica meteorite Y 82050, up to 62% of the Hg present in that sample was only released at temperature higher than 300 °C, suggesting strong contamination by Hg like halogens, and this may be the case for all Antarctica meteorites (Kumar et al., 2001). Therefore, high Hg concentrations reported for meteorites should be taken with care.

Thermal analysis of Hg-bearing chondrites have shown that the major proportion of Hg is released at relatively high temperature (>340 °C) is synchronous with S releasing temperature. This strongly suggests that HgS is the major Hg compound in these meteorites. The same thermal behavior has been shown for some other meteorites (e.g. Jovanovic and Reed, 1976; Kumar and Goel, 1992) and, recently, reported by Komorowski et al. (2012) who first characterized the presence of Hg–Cu-bearing metal-sulfide in an unshocked H-3 chondrite, Tieschitz meteorite.

The suggested amount of Hg brought in by the Chicxulub impact, even considering the large range of Hg content from 1 to 400 $ng \cdot g^{-1}$, would have contributed with 10 to 400 × $10^3$ tons of Hg. Although this could have increased the Hg spike at the KTB, as shown at the Stevns Klint profile, it could not account, by other mixing processes, for the increasing Hg content across the KTB, also shown in our profiles.

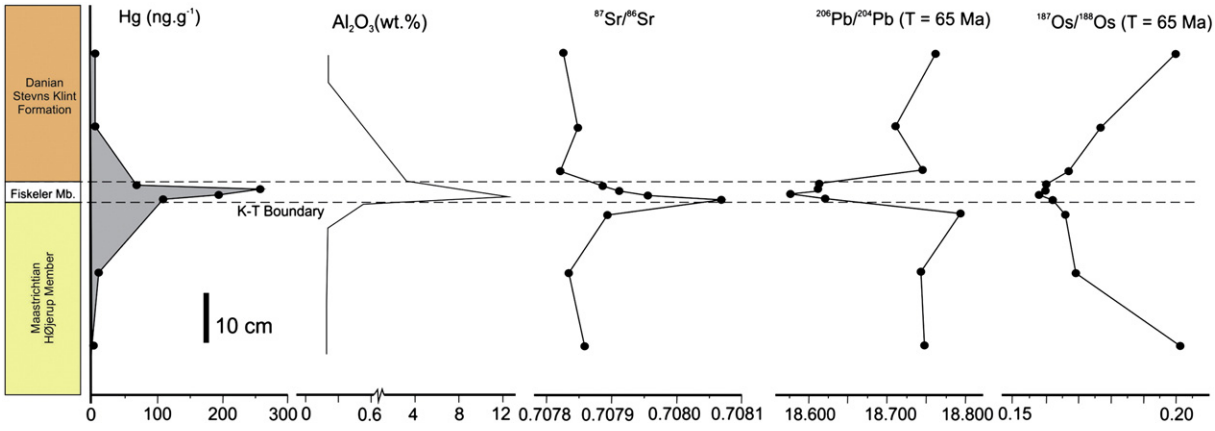


**Fig. 7.** Hg, $Al_2O_3$, $\delta^{13}C$ and $\delta^{18}O$ variation curves across the KTB at Stevns Klint, Denmark. $Al_2O_3$ curve is from Schmitz et al. (1992).

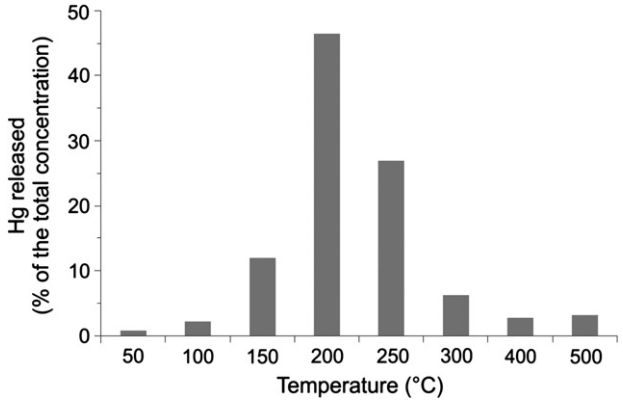


**Fig. 8.** Average Hg content released from sedimentary rocks of the Yacoraite Formation under different temperatures.

On the other hand, the much larger contribution from volcanic activity, such as that of the Deccan traps, could have increased worldwide Hg concentrations across the KTB.

The predominance of $Hg^{2+}$ in the analyzed samples in the present study, as suggested by the thermo-desorption experiment, therefore, supports a volcanic rather than a meteoritic source for the Hg.

Just as a matter of comparison, volcanism followed major Neoproterozoic glaciations supplying $CO_2$ to the atmosphere that led to greenhouse effect and further cap carbonate deposition in the aftermath of glaciations. Hg concentration linked to such volcanism can potentially be used as a test to investigate how volcanism could influence Hg background values. Sial et al. (2010) have reported Hg concentration levels in Neoproterozoic cap carbonates (~280 $ng \cdot g^{-1}$) equivalent to levels observed at Stevns Klint and in the Yacoraite Formation (~250 $ng \cdot g^{-1}$). This is perhaps an important information to the present discussion since volcanism, in the absence of known meteorite impacts, was the main Hg supplier to the Earth's surface during Neoproterozoic cap carbonate formation.

Isotopic composition of Hg is potentially one way to differentiate volcanogenic from meteoritic Hg. Characterization of the isotope composition of mantle-derived Hg is difficult because samples usually contain Hg that is either not entirely mantle-derived and/or because Hg has already undergone fractionation during chemical and phase transformations (Bergquist and Blum, 2009). Sherman et al. (2009) suggested that mantle-derived Hg might be isotopically heavier than crustal Hg, with $\delta^{202}Hg$ and $\Delta^{201}Hg$ values closer to 0‰. Zambardi et al. (2009) have found that $\delta^{202}Hg$ values from an active volcano in Italy range from −1.74‰ to −0.11‰ for gas and particulates, respectively. Most natural samples that obtained Hg after it had been through cycling in the environment have $\delta^{202}Hg$ values significantly different from crust and mantle values (Bergquist and Blum, 2009).

In summary, the current Hg isotope research is in its infancy. Just a very limited number of laboratories perform routinely Hg isotope-ratio analysis in the field of geosciences. It is necessary to generate a reliable Hg-isotope database to allow for a distinction between volcanogenic Hg and meteorite-derived Hg. Potentially, Hg isotopes may become a key in the solution of the role of meteorite impact versus volcanism as the cause of past global catastrophes and mass extinction.

As demonstrated by Kelley (2007), the relationship between mass extinctions, well-constrained ages for large igneous provinces, and hypervelocity impacts, tends to favor volcanic events, the well-known mass extinction of the KTB being the only one in which an impact coincides with a massive volcanic event. Perhaps this is the case in which an impact coeval with large volcanism has been underestimated as main cause of an extinction event — the KTB extinction.

All the conclusions stemming from this study are in consonance with volcanism playing an important role during extreme environmental turnover as witnessed at the KTB.

## Acknowledgments

We thank Gilsa M. Santana and Vilma S. Bezerra for assistance with stable isotope analyses in the LABISE and to Talita M. Soares for help with the Hg analysis. We are grateful to three anonymous reviewers whose comments and suggestions on an earlier version of the manuscript greatly contributed to improve it. This study was partially supported by the Paraíba Drilling Project/UFPE/CNPq/Princeton University and by grants to ANS (CNPq 470399/2008, CNPq 472842/2010-2, and FACEPE APQ 0727-1.07/08) to LDL (CNPq INCT-TMCOcean 573.601/2008-9) and to RAM (PIP-CONICET 200801-0061, CIUNSA 1680 and 2043 projects, Universidad Nacional de Salta). This is the NEG-LABISE contribution n. 259.

## References

Aberhan, M., Weidemeyer, S., Kiessling, W., Scasso, R.A., Medina, F.A., 2007. Faunal evidence for reduced productivity and uncoordinated recovery in Southern Hemisphere Cretaceous–Paleogene boundary sections. Geology 35, 227–230.
Alvarez, L.W., Alvarez, W., Asaro, F., Michael, H.V., 1980. Extraterrestrial cause for the Cretaceous–Tertiary extinction. Science 208, 1095–1108.
Archibald, J.D., et al., 2010. Cretaceous extinctions: multiple causes. Science 328, 973–976.
Barnes, H.L., Seward, T.M., 1997. Geothermal systems and mercury deposits. In: Barnes, H.L. (Ed.), Geochemistry of Hydrothermal Ore Deposits. John Wiley & Sons, New York, pp. 699–736.
Becker, L., Poreda, R.J., Hunt, A.G., Bunch, T.E., Rampino, M., 2001. Impact event at the Permian–Triassic boundary: evidence from extraterrestrial noble gases in fullerenes. Science 291, 1530–1533.
Beerling, D.J., Harfoot, M., Lomax, B., Pyle, J., 2007. The stability of the stratospheric ozone layer during the end-Permian eruption of the Siberian Traps. Philosophical Transactions of the Royal Society 365, 1843–1866.
Bergquist, B.A., Blum, J.D., 2009. The odds and evens of mercury isotopes: applications of mass-dependent and mass-independent isotope fractionation. Elements 5, 353–357.
Berner, A.R., 2002. Examination of hypotheses for the Permo–Triassic boundary extinction by carbon cycle modeling. Proceedings of the National Academy of Science 99, 4172–4177.
Bohor, B.F., 1990. Shocked quartz and more: impact signatures in Cretaceous/Tertiary boundary clays. Geological Society of America Special Paper 247, 335–342.
Bohor, B.F., Modreski, P.J., Foord, E.E., 1984. Shocked quartz in the Cretaceous–Tertiary boundary clays: evidence for a global distribution. Science 224, 705–709.
Campbell, I.H., Czamanske, G.K., Fedorenko, V.A., Hill, R.I., Stepanov, V., 1992. Synchronism of the Siberian Traps and the Permian–Triassic boundary. Science 258, 1760–1763.
Christensen, L., Fregerslev, S., Simonsen, A., Thiede, J., 1973. Sedimentology and depositional environment of Lower Danian Fish clay from Stevns Klint, Denmark. Bulletin of the Geological Society of Denmark 22, 193–212.
Claeys, P., Kiessling, W., Alvarez, W., 2002. Distribution of Chicxulub ejecta at the Cretaceous–Tertiary boundary. In: Koeberl, C., MacLeod, K.G. (Eds.), Catastrophic Events and Mass Extinctions: Impacts and Beyond. Boulder, Colorado, Geological Society of America Special Paper, 356, pp. 55–68.
Courtillot, V.E., Renne, P.R., 2003. On the ages of flood basalt events. Comptes Rendus, Geoscience 335, 113–140.
Denne, R.A., Scott, E.D., Eickhoff, D.P., Kaiser, J.S., Hill, R.J., Spaw, J.M., 2013. New evidence for widespread Chicxulub-induced slope failure Massive Cretaceous–Paleogene boundary deposit, deep-water Gulf of Mexico: new evidence for widespread Chicxulub-induced slope failure. Geology. http://dx.doi.org/10.1130/G34503.1.
Elliott, W.C., 1993. Origin of the Mg-smectite at the Cretaceous/Tertiary (K/T) boundary at Stevns Klint, Denmark. Clay Mineralogy 41, 442–452.
Frei, R., Frei, K.M., 2002. A multi-isotopic and trace element investigation of the Cretaceous–Tertiary boundary layer at Stevns Klint, Denmark: inferences for the origin and nature of siderophile and lithophile element geochemical anomalies. Earth and Planetary Science Letters 203, 691–708.
Gertsch, B., Keller, G., Adatte, T., Berner, A., 2013. The Cretaceous-Tertiary boundary (KTB) transition in NE Brazil. Journal of the Geological Society 170, 249–262.
Hansen, H.J., Gwozdz, R., Rasmussen, K.L., 1988. High-resolution trace element chemistry across the Cretaceous-Tertiary boundary in Denmark. Revista Española de Paleontología 21–29.
Hart, M.B., Feist, S.E., Price, G.D., Leng, M.J., 2004. Reappraisal of the K–T boundary succession at Stevns Klint, Denmark. Journal of the Geological Society of London 161, 1–8.
Hildebrand, A.R., Boynton, W.V., 1989. Hg anomalies at the K/T boundary: evidence for acid rain? Meteoritics 24, 277–278.

Hoffman, C., Feraud, G., Courtillot, V., 2000. $^{40}Ar/^{39}Ar$ dating of mineral separates and whole rocks from the Western Ghats lava pile: further constraints on duration and age of Deccan traps. Earth and Planetary Science Letters 180, 13–27.
Jovanovic, S., Reed Jr., G.W., 1976. $^{196}Hg$ and $^{202}Hg$ isotopic ratios in chondrites: revisited. Earth and Planetary Science Letters 31, 95–100.
Kamo, S., Lana, C., Morgan, J., 2011. U–Pb ages of shocked zircon grains link distal K–Pg boundary sites in Spain and Italy with the Chicxulub impact. Earth and Planetary Science Letters 310, 401–408.
Keller, G., 2005. Impacts, volcanism and mass extinction: random coincidence or cause and effect? Australian Journal of Earth Sciences 52, 725–757.
Keller, G., Stinnesbeck, W., Adatte, T., Stüben, D., 2003. Multiple impacts across the Cretaceous–Tertiary boundary. Earth-Science Reviews 62, 327–363.
Keller, G., Adatte, T., Tantawy, A.A., Berner, Z., Stinnesbeck, W., Stueben, D., Leanza, H.A., 2007. High stress late Maastrichtian e early Danian palaeoenvironment in the Neuquén Basin, Argentina. Cretaceous Research 28, 939–960.
Kelley, S., 2007. The geochronology of large igneous province, terrestrial impact craters, and their relationship to mass extinctions on Earth. Journal of the Geological Society 164, 923–936.
Komorowski, C.C., El Goresy, A., Miyahara, M., Boudouma, O., Ma, C., 2012. Discovery of Hg–Cu-bearing metal-sulfide assemblages in a primitive H-3 chondirte: towards a new insight in early solar system processes. Earth and Planetary Science Letters 349 (350), 261–271.
Krupp, R., 1988. Physicochemical aspects of mercury metallogenesis. Chemical Geology 69, 345–356.
Kumar, P., Goel, P.S., 1992. Variable $^{196}Hg/^{202}Hg$ ratio in stone meteorites and in some of their carbon-rich residues. Chemical Geology 102, 171–183.
Kumar, P., Ebihara, M., Bhattacharya, S.K., 2001. $^{196}Hg/^{202}Hg$ ratio and Hg content in meteorites and terrestrial standard rocks: a RNAA study. Geochemical Journal 35, 101–116.
Lauretta, D.S., Klaue, B., Blum, J.D., Buzek, P.R., 2001. Mercury abundances and isotopic compositions in the Murchison (CM) and Allende (CV) carbonaceous chondrites. Geochimica et Cosmochimica Acta 65, 2807–2818.
Lauridsen, B.W., Bjerager, M., Surlyk, F., 2012. The middle Danian Faxe Formation — new lithostratigraphic unit and a rare taphonomic window into the Danian of Denmark. Bulletin of the Geological Society of Denmark 60, 47–60.
Machalski, M., Heinberg, C., 2005. Evidence for ammonite survival into the Danian (Paleogene) from the Cerithium Limestone at Stevns Klint, Denmark. Bulletin of the Geological Society of Denmark 52, 97–111.
Marquillas, R.A., Salfity, J.A., 1988. Tectonic framework and correlations of the Cretaceous–Eocene Salta Group, Argentine. In: Bahlburg, H., Breitkreuz, C., Giese, P. (Eds.), The Southern Central Andes: Contributions to Structure and Evolution of an Active Continental Margin. Lecture Notes in Earth Sciences, 17. Springer-Verlag, Berlin, pp. 119–136.
Marquillas, R.A., del Papa, C.E., Sabino, I.F., Heredia, J., 2003. Prospección del límite K/T en la cuenca del Noroeste, Argentina. Revista de la Asociación Geológica Argentina 58, 271–274.
Marquillas, R.A., del Papa, C.E., Sabino, I., 2005. Sedimentary aspects and paleoenvironmental evolution of a rift basin: Salta Group (Cretaceous–Paleogene), northwestern Argentina. International Journal of Earth Sciences 94, 94–113.
Marquillas, R.A., Sabino, I., Sial, A.N., del Papa, C., Ferreira, V., Matthews, S., 2007. Carbon and oxygen isotopes of Maastrichtian–Danian shallow marine carbonates: Yacoraite Formation, northwestern Argentina. Journal of South American Earth Sciences 23, 304–320.
Marquillas, R.A., Salfity, J.A., Matthews, S.J., Matteini, M., Dantas, E., 2011. U–Pb zircon age of the Yacoraite Formation and its significance to the Cretaceous–Tertiary boundary in the Salta Basin, Argentina. In: Salfity, J.A., Marquillas, R.A. (Eds.), Cenozoic Geology of the Central Andes of Argentina. SCS Publisher, pp. 227–246.
Martínez-Cortizas, A., Pontevedra-Pombal, X., García-Rodeja, E., Nóvoa-Muñoz, J.C., Shotyk, W., 1999. Mercury in a Spanish Peat Bog: archive of climate change and atmospheric metal deposition. Science 284, 939–942.
Morgan, J.V., Lana, C., Kearsley, A., Coles, B., Belcher, C., Montanari, S., Díaz-Martínez, E., Barbosa, J.A., Neumann, V., 2006. Analyses of shocked quartz at the global K–P boundary indicate an origin from a single, high-angle, oblique impact at Chicxulub. Earth and Planetary Science Letters 251, 264–279.
Morrison, D., 2004. Did an Impact Trigger the Permian–Triassic Extinction? NASA Astrobilogy Institute (NAI) (May 17, 2004).
Nascimento-Silva, V.M., Sial, A.N., Ferreira, V.P., Neumann, V.H., Barbosa, J.A., Pimentel, M.M., Lacerda, L.D., 2011. Cretaceous–Paleogene transition at the Paraíba Basin, northeastern, Brazil: carbon-Isotope and mercury subsurface stratigraphies. Journal of South American Earth Sciences 32, 379–392.
Neumann, V.H., Barbosa, J.A., Nascimento-Silva, M.V., Sial, A.N., Lima-Filho, M.L., 2009. Sedimentary development and isotope analysis of deposits at the Cretaceous/Paleogene transition in the Paraíba basin, NE Brazil. Poland. Geologos 2, 103–113.
Nriagu, J.O., Becker, C., 2003. Volcanic emissions of mercury to the atmosphere: global and regional inventories. The Science of the Total Environment 304, 3–12.
Ozerova, N.A., Kvasha, L.G., Bulkin, G.A., Aidinian, N.Kh., 1973. Certain peculiarities in the distribution of mercury in meteorites. Geochimica et Cosmochimica Acta 37, 569–582.
Palinkaš, A.L., Drobne, K., Durn, G., Miko, S., 1996. Mercury anomaly at the Cretaceous–Tertiary boundary: Dolenja Vas, Slovenia. In: Drobne, K., Goričan, Š., Kotnik, B. (Eds.), Int. Workshop Postojna '96. The Role of Impact Processes in the Geological and Biological Evolution of Planet Earth, pp. 31–32.
Pimentel, M.M., Carmo, I., Terra, G., 2012. U–Pb age of tuffs from the Balbuena Group, Salta Basin, NW Argentina. VIII South American Symposium of Isotope Geology (SSAGI), Medellin, Colombia (CD-ROM).
Pyle, D.M., Mather, T.A., 2003. The importance of volcanic emissions for the global atmospheric mercury cycle. Atmospheric Environment 37, 5115–5124.
Randa, Z., Kucera, L., Soukal, L., 2003. Elemental characterization of the new Czech meteorite Morávka by neutron and photon activation analysis. Journal of Radioanalytical and Nuclear Chemistry 257, 275–283.
Renne, P.R., Black, Michael T., Zichao, Z., Richards, M.A., Basu, A.R., 1995. Synchrony and causal relations between Permian–Triassic boundary crises and Siberian flood Volcanism. Science 269, 1413–1416.
Roos-Barraclough, F., Shotyk, W., 2003. Millennial-scale records of atmospheric mercury deposition obtained from ombrotrophic and minerotrophic peatlands in the Swiss Jura Mountains. Environmental Science & Technology 37, 235–244.
Roos-Barraclough, F., Martinez-Cortizas, A., García-Rodeja, E., Shotyk, W., 2002. A 14 500 year record of the accumulation of atmospheric mercury in peat: volcanic signals, anthropogenic influences and a correlation to bromine accumulation. Earth and Planetary Science Letters 202, 435–451.
Rytuba, J.J., 2005. Geogenic and mining sources of mercury to the environment. In: Parsons, M.B., Percival, J.B. (Eds.), Mercury: Sources, Measurement, Cycles and Effects. Mineralogical Association of Canada — Short Course Series, 34, pp. 21–41.
Salfity, J.A., Marquillas, R.A., 1994. Tectonic and Sedimentary Evolution of the Cretaceous–Eocene Salta Group basin, Argentina. In: Salfity, J.A. (Ed.), Cretaceous tectonics of the Andes: Braunschweig/Weisbaden, Earth Evolution Sciences Monograph Series. Friedr. Vieweg & Sohn, pp. 266–315.
Salfity, J.A., Monaldi, C.R., Guidi, F., Sales, R.J., 1998. Mapa geológico de la Província de Salta: Buenos Aires, Secretaría de Industria, Comercio y Minería, Servício Geológico Argentino, scale: 1:500,000.
Sanei, H., Grassby, S.E., Beauchamp, B., 2012. Latest Permian mercury anomalies. Geology 40, 63–66.
Santos, G.M., Cordeiro, R.C., Silva Filho, E.V., Turcq, B., Lacerda, L.D., Fifield, L.K., Gomes, P.R.S., Hauscaden, P.A., Sifeddine, A., Albuquerque, A.L.S., 2001. Chronology of the atmospheric mercury in Lagoa da Pata Basin, Upper Rio Negro of Brazilian Amazon. Radiocarbon 43, 801–808.
Scasso, R., Concheyro, A., Kiessling, W., Aberhan, M., Hecht, L., Medina, F., Tagle, R., 2005. A tsunami deposit at the Cretaceous/Paleogene boundary in the Neuquén Basin of Argentina. Cretaceous Research 26, 283–297.
Schmitz, B., 1985. Metal precipitation in the Cretaceous–Tertiary boundary clay at Stevns Klint, Denmark. Geochimica et Cosmochimica Acta 49, 2361–2370.
Schmitz, B., Andersson, P., Dahl, J., 1988. Iridium, sulfur isotopes and rare earth elements in the Cretaceous–Tertiary boundary clay at Stevns Klint, Denmark. Geochimica et Cosmochimica Acta 52, 229–236.
Schmitz, B., Keller, G., Stenvall, O., 1992. Stable isotope and foraminiferal changes across the Cretaceous–Tertiary boundary at Stevns Klint, Denmark: arguments for long-term oceanic instability before and after bolide-impact event. Palaeogeography, Palaeoclimatology, Palaeoecology 96, 233–260.
Sherman, L.S., Blum, J.D., Nordstrom, D.K., McCleskey, R.B., Barkay, T., Vetriani, C., 2009. Mercury isotopic composition of hydrothermal systems in the Yellowstone Plateau volcanic field and Guaymas Basin sea-floor rift. Earth and Planetary Science Letters 279, 86–96.
Sheth, H.C., 2005. Were the Deccan flood basalts derived in part from ancient oceanic crust within the Indian continental lithosphere? Gondwana Research 8, 109–127.
Shima, M., Jochum, K.P., Sighnolfi, G.P., Hinteberger, H.H., 1974. The chemical composition of major elements and heavy trace metals in chondrites Parambu and Marilia. Meteoritics 9, 199–207.
Shukolyukov, A., Lugmair, G.W., 1998. Isotopic evidence for the Cretaceous–Tertiary impactor and its type. Science 282, 927–929.
Sial, A.N., Ferreira, V.P., Toselli, A.J., Parada, M.A., Agenolaza, F.G., Pimentel, M.M., Alonso, R.N., 2001. Carbon and oxygen isotope compositions of some Upper Cretaceous–Paleocene sequences in Argentina and Chile. International Geology Review 43, 893–909.
Sial, A.N., Gaucher, C., Silva Filho, M.A., Ferreira, V.P., Pimentel, M.M., Lacerda, L.D., Silva Filho, E.V., Cezario, W., 2010. C-, Sr-isotope and Hg stratigraphies of Neoproterozoic cap carbonates of the Sergipano Belt, Northeastern Brazil. Precambrian Research 182, 351–372.
Smit, J., 1999. The global stratigraphy of the Cretaceous–Tertiary boundary impact ejecta. Annual Review of Earth and Planetary Science 27, 75–113.
Smit, J., Klaver, G., 1981. Sanidine spherules at the Cretaceous–Tertiary boundary indicate a large impact event. Nature 292, 47–49.
Smith, C.N., Kesler, S.E., Blum, J.D., Rytuba, J.R., 2008. Isotope geochemistry of mercury in source rocks, mineral deposits and spring deposits of the California Coast Ranges, USA. Earth and Planetary Science Letters 269, 399–407.
Stinnesbeck, W., Keller, G., 1996. Environmental changes across the Cretaceous–Tertiary boundary in Northeastern Brazil. In: MacLeod, N., Keller, G. (Eds.), Cretaceous–Tertiary Mass Extinctions: Biotic and Environmental Changes. W.W. Norton and Company, New York, p. 575.
Stüben, D., Kramar, U., Harting, M., Stinnesbeck, W., Keller, G., 2005. High-resolution geochemical record of Cretaceous–Tertiary boundary sections in Mexico: new constraints on the K/T and Chicxulub events. Geochimica et Cosmochimica Acta 69, 2559–2579.
Surlyk, F., Damholt, T., Bjerager, M., 2006. Stevns Klint, Denmark: Uppermost Maastrichtian chalk, Cretaceous–Tertiary boundary, and lower Danian bryozoans mound complex. Bulletin of the Geological Society of Denmark 54, 1–48.
Swisher III, C.C., Grajales-Nishimura, J.M., Montanari, A., Margolis, S.V., Claeys, P., Alvarez, W., Renne, P., Cedillo-Pardoa, E., Maurrasse, F.J.-M., Curtis, G.H., Smit, J., McWilliams, M.O., 1992. Coeval $^{40}Ar/^{39}Ar$ ages of 65.0 Million years ago from Chicxulub Crater Melt Rock and Cretaceous–Tertiary Boundary Tektites. Science 257, 954–958.
Valle, C.M., Santana, G., Augusti, R., Egreja, F.B., Windmoeller, C.C., 2005. Speciation and quantification of mercury in Oxisol, Ultisol and Spodosol from Amazon (Manaus, Brazil). Chemosphere 58, 779–792.

Vandal, G.M., Fitzgerald, W.F., Boutron, C.F., Candelon, J.P., 1993. Nature 362, 621.
Varekamp, J.C., Buseck, P.R., 1986. Global mercury flux from volcanic and geothermal sources. Applied Geochemistry 1, 65–73.
Varekamp, J.C., Waibel, A.F., 1987. Natural cause for pollution at Clear Lake, California, and paleotectonic inferences. Geology 15, 1018–1021.
Wignall, P.B., 2001. Large igneous province and mass extinctions. Earth-Science Reviews 53, 1–33.
Zambardi, T., Sonke, J.E., Toutain, J.P., Sortinob, F., Shinoharac, H., 2009. Mercury emissions and stable isotopic compositions at Vulcano Island (Italy). Earth and Planetary Science Letters 277, 236–243.